

## Design of Tire Fault Observer Based on Estimation of Tire/Road Friction Conditions<sup>1)</sup>

LI Li<sup>1,3</sup> WANG Fei-Yue<sup>1,3</sup> SHAN Guo-Ling<sup>2</sup> ZHOU Qun-Zhi<sup>1</sup>

<sup>1</sup>(Laboratory of Complex Systems and Intelligent Science, Institute of Automation, Chinese Academy of Sciences, Beijing 100080)

<sup>2</sup>(Triangle Tire Corporation, Ltd, WeiHai, Shandong 210016)

<sup>3</sup>(The Program for Advanced Research in Complex Systems, The University of Arizona, Tucson, Arizona, USA)  
(E-mail: lil@email.arizona.edu)

**Abstract** Many tire fault monitors are designed nowadays because tire failure is proved to be one of the main causes of traffic accidents. However, most of them are of high manufacturing cost and unreliable. A new practical tire fault observer is devoted. Based on the introduced dynamic tire/road friction model that considers external disturbances, the observer estimates and tracks the changes of tire/road friction conditions using vehicle track forces and wheel angular velocity information to carry out tire fault diagnosis. Since the wheel speed sensor is a basic component of normal anti-lock brake system (ABS), the observer proposed could be easily realized in low cost within the anti-lock brake system.

**Key words** Tire/road friction estimation, nonlinear observer, strong practically stable, fault observer

### 1 Introduction

Nowadays, people find out that many traffic accidents, especially some really bad ones, are caused by tire failure. Therefore, to measure and monitor the tire and ensure the road surface friction in a cruising state well within the safe limit is important. In the last decade, there were numerous papers on it. One basic way to solve this problem is to model tire/road friction and to estimate the related parameters online so as to monitor the state of the tire indirectly. The most often used description of the tire/road model is a set of curves of the wheel slip with which the normalized friction force is defined. And based on it, the tire/road friction condition could be analyzed<sup>[1,2]</sup>.

In this field, the two analytical models presented by Bakker *et al.*<sup>[3]</sup> are often used by researchers. In these two models,  $\mu = F/F_n$  (where  $F$  denotes the Friction force and  $F_n$  denotes the normal force) is mainly determined by the wheel slip  $s$  with regard to some other parameters such as speed. Here  $s$  is defined as

$$s = \begin{cases} 1 - \frac{r\omega}{v}, & \text{if } v > r\omega, v \neq 0, \text{ braking} \\ 1 - \frac{v}{r\omega}, & \text{if } v < r\omega, \omega \neq 0, \text{ driving} \end{cases}$$

where  $r$  is the radius of the wheel,  $\omega$  is the angular velocity,  $v$  is the longitudinal velocity.

The two curves shown in the following Fig. 1, which are obtained by Harned *et al.*<sup>[4]</sup>, demonstrate the typical relation between  $\mu$  and  $s$  under different road conditions. However, this model lacks a physical interpretation and it is difficult to put into use for too many parameters are underdetermined.

1) Supported by the Outstanding Overseas Chinese Scholars Fund of Chinese Academy of Sciences, the National Outstanding Youth Research Programme of P. R. China, and Triangle Tire Corporation, Ltd

Received November 1, 2002; in revised form March 13, 2003

收稿日期 2002-11-01; 收修改稿日期 2003-03-13

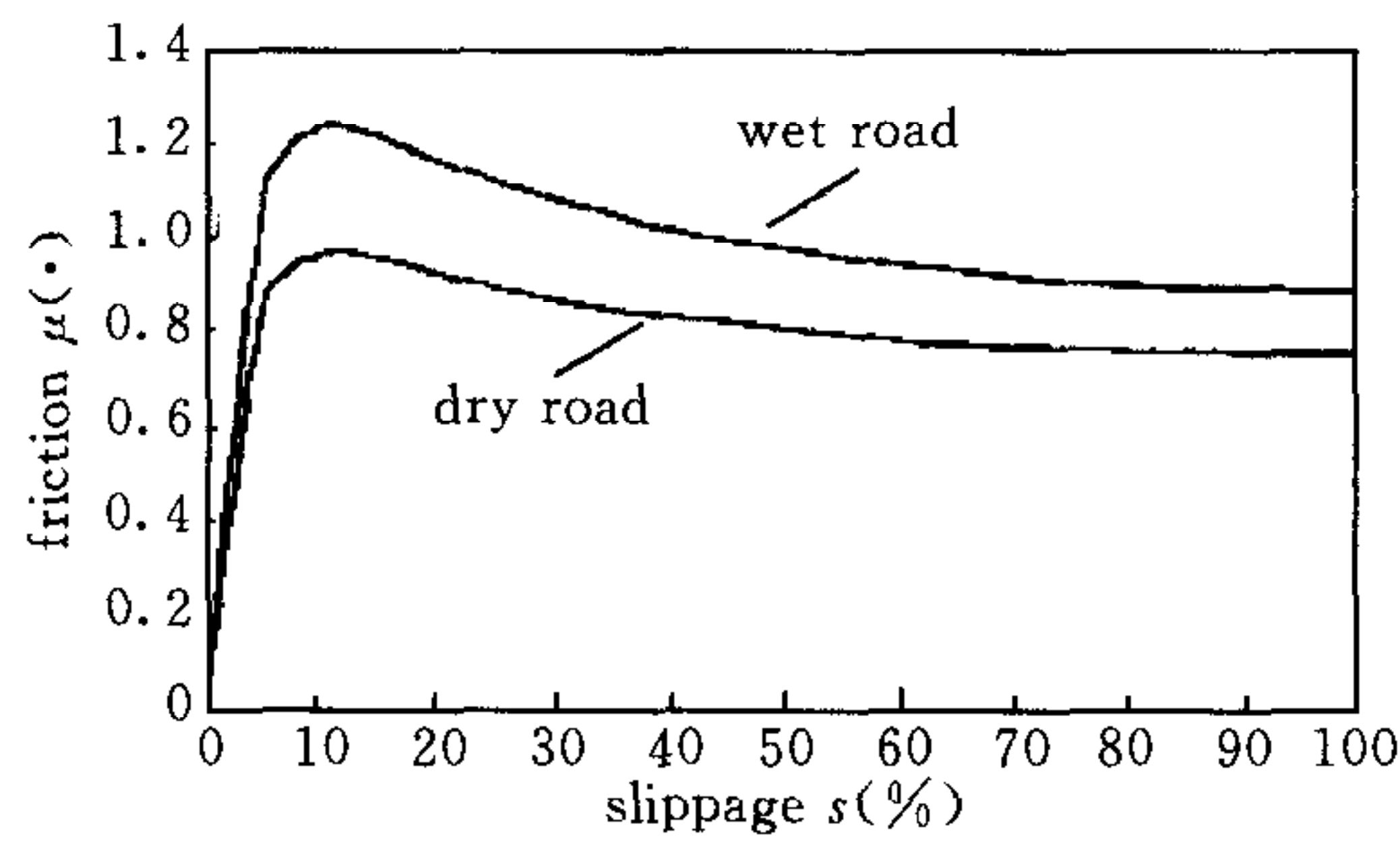


Fig. 1 Relationship between coefficient of road adhesion  $\mu$  and longitudinal slip  $s$  for different road surface conditions<sup>[2]</sup>

Recently, dynamic friction models, such as the one presented by Candudas de Wit *et al.* in [5], have been proposed successfully to identify and compensate for the friction in mechanical systems. In [6] Candudas de Wit *et al.* used the so called LuGre model to estimate a parameter in the model that reflects changes in the tire/road characteristics for the first time. In this paper, both the angular and longitudinal velocities are assumed to be measurable. Since in some application the longitudinal velocity cannot be obtained, it is necessary to design an observer to estimate the slip ratio using the angular information only. In [7] and [8], Candudas de Wit, Jingang Yi, *et al.* formulated the model together with a new nonlinear observer to solve this problem.

This paper is devoted to extending the approach of [7] and [8] in two ways. First, the inevitable disturbance of the model parameter is considered in the model since the actual road condition parameter should be varied within a certain range for a certain time. Second, a proper fault detection rule should be set associated with the system when it is used as a fault observer. In order to achieve these two goals, a modified model is proposed and a novel fault observer for the tire/road contact friction is constructed based on strong practically stable theory. The rest of this paper is arranged as follows: Section 2 brings forward the formulations of the observer problem; Section 3 presents how to construct the fault observer and its basic characteristics; Section 4 provides some simulation results to show the feasibility of this approach; finally Section 5 concludes the paper.

## 2 Problem formulation

A potential advantage of such models is their ability to describe closely some of the physical phenomena found in road/tire friction (i. e. hysteresis loops, pre-sliding displacement, etc), and to depend on a parameter directly related with the phenomena to be observed, for instance, the change on the road characteristics (i. e. dry or wet). Dynamic models can be formulated as a lumped or distributed ones.

The lumped friction model proposed by Canudas-de-Wit and Tsiotras<sup>[6]</sup> is based on a similar dynamic friction model for contact-point friction problems developed previously, which is called LuGre model. The model given below has been proved to be a good approximation of distributed tire/road friction models that are able to represent the typical characteristics as the ones displayed by Fig. 1.

$$\dot{z} = -v_r - \theta \frac{\sigma_0 |v_r|}{g(v_r)} z \quad (1)$$

$$F = (\sigma_0 z + \sigma_1 \dot{z} - \sigma_2 v_r) F_n \quad (2)$$

with  $g(v_r) = \mu_c + (\mu_s - \mu_c) e^{-|v_r/v_s|^{1/2}}$  where  $\sigma_0$  is the rubber longitudinal stiffness,  $\sigma_1$  is the rubber longitudinal damping,  $\sigma_2$  is the viscous relative damping,  $\mu_s$  is the normalized static friction coefficient, and  $\mu_c$  is the normalized Coulomb friction.  $v_s$  is the Stribeck relative

velocity,  $F_n$  is the normal force, and  $v_r = v - r\omega$  is the relative velocity.  $z$  is an introduced parameter denoting the internal friction state. Surfaces are very irregular at the microscopic level and two surfaces therefore make contact at a number of asperities. It could be viewed as two rigid bodies that make contact though elastic bristles.  $z$  could be viewed as the average deflection of those bristles.

Here,  $\theta$  is an undetermined parameter of the tire/road condition on which we focus in this paper. It will change with the variation of the road condition if the tire condition does not change. Under normal tire pressure, some typical data of it is: for dry asphalt conditions,  $\theta=1$ ; for wet asphalt conditions,  $\theta=2.5$  and for snow conditions,  $\theta=4$ . The abnormal tire pressure will lead to significant variation of  $\theta$ .

In most of the previous works, no disturbance is considered in the modeling process. However, the road condition could not be ideal and should be varied within a certain range. In this paper, we model all the disturbance into the variation of  $\theta$  as the following

$$\dot{\theta} = \epsilon \tag{3}$$

where  $\epsilon$  represents the certain stable stochastic disturbance process. Since the highway road condition does not vary abruptly, without loss of generality, we could assume this disturbance satisfies:

1)  $\epsilon$  is bounded as  $|\epsilon| \leq \tau, \tau > 0$ ;

2)  $\theta$  is bounded, i. e.  $|\theta - \bar{\theta}| = \left| \theta_0 + \int_0^t \epsilon d\tau - \bar{\theta} \right| \leq \Delta\theta_{\max}$ , where  $\theta_0$  denotes the initial value of  $\theta$  and  $\bar{\theta}$  denotes the expectation of  $\theta$ .

The values of  $\tau$  and  $\Delta\theta_{\max}$  should be determined by actual environment. From practical tests, we could see that these values are normally small. So estimating and monitoring the value of  $\theta$  could detect a fault if the value of  $\theta$  becomes especially abnormal. In the following parts, we will see how to design a fault observer for  $\theta$  and how to get a fault detection rule. Before further discussion, let's review some basic properties of this model.

**Remark 1.** the model has the following important properties:

i)  $1 \geq \mu_s \geq g(v_r) \geq \mu_c \geq 0, \forall v_r \in R$ ;

ii)  $f(v_r) = \frac{|v_r|}{g(v_r)}$  is positive and bounded and  $f'(v_r)$  is also bounded, i. e.,  $0 \leq f(v_r) \leq \rho_1, 0 \leq |f'(v_r)| \leq \rho_2, \forall v_r \in R$ .

Considering the lumped tire/road friction model together with velocity dynamics, the estimation model can be formulated as follows

$$m\dot{v} = 4F - \sigma_v m g v \tag{4}$$

$$J\dot{\omega} = -rF - u_T \tag{5}$$

where  $J$  and  $m$  are the inertia and 1/4 mass of the wheel, respectively. The term  $\sigma_v$  is the rolling resistance coefficient and  $g$  is the gravity constant.

Assume that only the variable  $\omega$  is measurable, and the lumped friction parameters with  $\theta=1$  have been identified offline (see Table 1 for sample data from Triangle Tire Corporation).

Table 1 Sample data of the off-line identification for LuGre Model

Parameter	Value	Unit
$\sigma_0$	25.0	1/m
$\sigma_1$	5.0	s/m
$\sigma_2$	0.1	s/m
$\mu_c$	0.5	—
$\mu_s$	0.9	—
$v_s$	12.5	m/s

### 3 Observer design

Let's introduce the same transform of coordinates in [5]:  $x_1 = \sigma z$ ,  $x_2 = v$ ,  $x_3 = v_r = v - r\omega$ . Then we can get

$$\dot{x}_1 = \sigma_0 \dot{z} = -\sigma_0 x_3 - \sigma_0 \theta \frac{|x_3|}{g(x_3)} x_1 \quad (6)$$

$$\dot{x}_2 = g[x_1 + \sigma_1 \left(-x_3 - \theta \frac{|x_3|}{g(x_3)} x_1\right) - \sigma_2 x_3] - g\sigma_v x_2 \quad (7)$$

$$\dot{x}_3 = \dot{v} - r\dot{\omega} = \alpha[x_1 + \sigma_1 \left(-x_3 - \theta \frac{|x_3|}{g(x_3)} x_1\right) - \sigma_2 x_3] - g\sigma_v x_2 + u_T \quad (8)$$

where  $\alpha = g\left(1 + \frac{mr^2}{4J}\right)$ .

Define  $\mathbf{x}$ ,  $y$  respectively as  $\mathbf{x} = [x_1 \ x_2 \ x_3]^T$ ,  $y = \frac{1}{r}(x_2 - x_3) = \omega$ , and introduce  $\varphi(\mathbf{x}) = \frac{|x_3|}{g(x_3)} x_1$ . Then we could rewrite the system as

$$\dot{\mathbf{x}} = \mathbf{A}\mathbf{x} + \mathbf{B}\theta\varphi(\mathbf{x}) + \mathbf{E}u_T \quad (9)$$

$$y = \mathbf{C}\mathbf{x} \quad (10)$$

where  $\mathbf{A} = \begin{bmatrix} 0 & 0 & -\sigma_0 \\ -g & -g\sigma_v & -g(\sigma_1 + \sigma_2) \\ \alpha & -g\sigma_v & -\alpha(\sigma_1 + \sigma_2) \end{bmatrix}$ ,  $\mathbf{B} = \begin{bmatrix} -\sigma_0 \\ -g\sigma_1 \\ -\alpha\sigma_1 \end{bmatrix}$ ,  $\mathbf{C} = \begin{bmatrix} 0 & \frac{1}{r} & -\frac{1}{r} \end{bmatrix}$ ,  $\mathbf{E} = \begin{bmatrix} 0 \\ 0 \\ 1 \end{bmatrix}$ .

Notice that  $(\mathbf{A}, \mathbf{C})$  is an observer pair, we can introduce the observer feedback matrix  $L$  and obtain the following observer structure which is like the ones proposed in [6] and [8]:

$$\dot{\hat{\mathbf{x}}} = \mathbf{A}\hat{\mathbf{x}} + \mathbf{B}\hat{\theta}\varphi(\hat{\mathbf{x}}) - L(y - \hat{y}) + k\mathbf{B}\text{sgn}(y - \hat{y}) + \mathbf{E}u_T \quad (11)$$

$$\dot{\hat{\theta}} = \gamma_1 \varphi(\hat{\mathbf{x}})(y - \hat{y}) \quad (12)$$

$$\hat{y} = \mathbf{C}\hat{\mathbf{x}} \quad (13)$$

where  $k = \max_x \{2\theta_{\max} |\varphi(\mathbf{x})|\}$ . From the above, we have  $k < \infty$ . And  $\gamma_1$  is a positive real number that is introduced to adjust the variation rate of  $\hat{\theta}$ .

From the above observer, we can get the dynamics of the estimated error as

$$\dot{\mathbf{x}}_e = \dot{\mathbf{x}} - \dot{\hat{\mathbf{x}}} = [\mathbf{A} + \mathbf{L}\mathbf{C}]\mathbf{x}_e + \mathbf{B}[\theta\varphi(\mathbf{x}) - \hat{\theta}\varphi(\hat{\mathbf{x}})] - k\mathbf{B}\text{sgn}(y_e) \quad (14)$$

$$\dot{\theta}_e = \dot{\theta} - \dot{\hat{\theta}} = \varepsilon - \gamma_1 \varphi(\hat{\mathbf{x}}) y_e \quad (15)$$

$$y_e = y - \hat{y} = \mathbf{C}\mathbf{x}_e \quad (16)$$

Before we reach the main results, let us introduce the Definition of the strong practically stable and a useful lemma.

**Definition.** If the solution of the dynamic system  $\begin{cases} \dot{\mathbf{x}} = f(t, \mathbf{x}) \\ \mathbf{x}(t_0) = \mathbf{x}_0 \end{cases}$  exists for any initial value  $\mathbf{x}(t_0) = \mathbf{x}_0$  during  $(t_0, \infty)$ , and there exist a positive real number  $d$  and a time  $t_d > 0$  such that the solution satisfies  $\|\mathbf{x}(t)\| \leq d$ , for any  $t \geq t_d$ , this system is said to be strong practically stable with respect to  $d$ . Here  $\|\mathbf{x}\|$  denotes  $\text{ess. sup.}\{|\mathbf{x}|\}$ .

**Lemma 1**<sup>[11,12]</sup>. The dynamic system described in Definition 1 is strong practical stable with respect to  $d_0 = (r_1^{-1} \cdot r_2)(c)$ , if there exist a first-order derivable positive function  $V(\cdot): \mathbb{R}^n \times \mathbb{R} \rightarrow \mathbb{R}^+$ , a continuous positive infinity function  $r_i(\cdot): \mathbb{R}^+ \rightarrow \mathbb{R}^+$ ,  $i=1,2$ , and a positive infinity function  $r_3(\cdot): \mathbb{R}^+ \rightarrow \mathbb{R}^+$  satisfying: a) there exists a positive real number  $c$  such that  $r_3(\|\mathbf{x}\|) > 0$  for any  $x > c$  and  $r_3(\|c\|) = 0$ ; b)  $r_1(\|\mathbf{x}\|) \leq V(x, t) \leq r_2(\|\mathbf{x}\|)$ ; c)  $\frac{\partial V(\mathbf{x}, t)}{\partial t} = \nabla_x V(\mathbf{x}, t) \cdot f(\mathbf{x}, t) \leq -r_3(\|\mathbf{x}\|)$ .

With this representation we shall now verify the following theorem under the assumed condition.

**Theorem 1.** The observer error state system designed above is strong practically stable with respect to  $\bar{d} = \sqrt{\frac{\lambda_{\max}(P) \cdot 4 |\theta_e|_{\max} \tau + 4 |\theta_e|_{\max}^2}{\lambda_{\min}(P) \cdot \lambda_{\min}(Q)}} \cdot \frac{\gamma_2}{\gamma_1}$ , when there exist positive symmetric matrix  $P$  and  $Q$  satisfying the following equations

$$-Q = [A + LC]^T P + P[A + LC] \quad (17)$$

$$PB = \gamma_2 C^T \quad (18)$$

where  $\gamma_2$  is a positive weighted number.

**Proof.** Consider the Lyapunov function  $V(t, \mathbf{x}) = \mathbf{x}_e^T P \mathbf{x}_e + \frac{\gamma_2}{\gamma_1} \theta_e^2$ . Since

$\theta\varphi(\mathbf{x}) - \hat{\theta}\varphi(\hat{\mathbf{x}}) = [\theta\varphi(\mathbf{x}) - \theta\varphi(\hat{\mathbf{x}})] + [\theta\varphi(\hat{\mathbf{x}}) - \hat{\theta}\varphi(\hat{\mathbf{x}})] = \theta[\varphi(\mathbf{x}) - \varphi(\hat{\mathbf{x}})] + \theta_e\varphi(\hat{\mathbf{x}})$   
we have

$$\begin{aligned} \dot{V} &= \mathbf{x}_e^T \{ [A + LC]^T P + P[A + LC] \} \mathbf{x}_e - k \mathbf{x}_e^T P B \operatorname{sgn}(y_e) - k [B \operatorname{sgn}(y_e)]^T P \mathbf{x}_e + \\ &\quad \mathbf{x}_e^T P B [\theta\varphi(\mathbf{x}) - \hat{\theta}\varphi(\hat{\mathbf{x}})] + [\theta\varphi(\mathbf{x}) - \hat{\theta}\varphi(\hat{\mathbf{x}})]^T B^T P \mathbf{x}_e + 2 \frac{\gamma_2}{\gamma_1} \theta_e [\varepsilon - \gamma_1 \varphi(\hat{\mathbf{x}}) y_e] = \\ &\quad \mathbf{x}_e^T \{ [A + LC]^T P + P[A + LC] \} \mathbf{x}_e - 2k\gamma_2 y_e \operatorname{sgn}(y_e) + \\ &\quad 2\gamma_2 y_e [\theta\varphi(\mathbf{x}) - \hat{\theta}\varphi(\hat{\mathbf{x}})] + 2 \frac{\gamma_2}{\gamma_1} \theta_e [\varepsilon - \gamma_1 \varphi(\hat{\mathbf{x}}) y_e] = \\ &\quad \mathbf{x}_e^T \{ [A + LC]^T P + P[A + LC] \} \mathbf{x}_e + 2\gamma_2 y_e \{ [\theta\varphi(\mathbf{x}) - \hat{\theta}\varphi(\hat{\mathbf{x}})] + \theta_e \varphi(\hat{\mathbf{x}}) \} - \\ &\quad 2k\gamma_2 y_e \operatorname{sgn}(y_e) - 2\gamma_2 \theta_e \varphi(\hat{\mathbf{x}}) y_e + 2 \frac{\gamma_2}{\gamma_1} \theta_e \varepsilon = \\ &\quad \mathbf{x}_e^T \{ [A + LC]^T P + P[A + LC] \} \mathbf{x}_e + 2\gamma_2 \theta [\varphi(\mathbf{x}) - \varphi(\hat{\mathbf{x}})] y_e - \\ &\quad 2k\gamma_2 y_e \operatorname{sgn}(y_e) + 2 \frac{\gamma_2}{\gamma_1} \theta_e \varepsilon \end{aligned}$$

Based on the assumption, we have

$$|\theta[\varphi(\mathbf{x}) - \varphi(\hat{\mathbf{x}})]| \leq \theta_{\max} [|\varphi(\mathbf{x})| + |\varphi(\hat{\mathbf{x}})|] \leq 2k$$

Thus

$$2\gamma_2 \theta [\varphi(\mathbf{x}) - \varphi(\hat{\mathbf{x}})] y_e - 2k\gamma_2 y_e \operatorname{sgn}(y_e) \leq 0$$

And since  $|\varepsilon| \leq \tau$ , we can have

$$\dot{V} \leq \mathbf{x}_e^T \{ [A + LC]^T P + P[A + LC] \} \mathbf{x}_e + 4 \frac{\gamma_2}{\gamma_1} |\theta_e|_{\max} \tau$$

From (17), we have

$$\dot{V} \leq -\lambda_{\min}(Q) \|\mathbf{x}_e\|^2 + 4 \frac{\gamma_2}{\gamma_1} |\theta_e|_{\max} \tau$$

Choose  $r_1(\|\mathbf{x}_e\|) = \lambda_{\min}(P) \|\mathbf{x}_e\|^2$ ,  $r_2(\|\mathbf{x}_e\|) = \lambda_{\max}(P) \|\mathbf{x}_e\|^2 + 4 \frac{\gamma_2}{\gamma_1} |\theta_e|_{\max}^2$

$$r_3(\|\mathbf{x}_e\|) = \lambda_{\min}(Q) \|\mathbf{x}_e\|^2 - 4 \frac{\gamma_2}{\gamma_1} |\theta_e|_{\max} \tau$$

Then based on Lemma 1, the observer error state system is strong practically stable with respect to

$$\bar{d} = \sqrt{\frac{\lambda_{\max}(P) \cdot 4 |\theta_e|_{\max} \tau + 4 |\theta_e|_{\max}^2}{\lambda_{\min}(P) \cdot \lambda_{\min}(Q)}} \cdot \frac{\gamma_2}{\gamma_1}$$

Based on this result, if the tire is in the steady state, the observer output error should be bounded, i. e.,

$$|y - \hat{y}| = \left| \frac{1}{r} [(x_2 - \hat{x}_2) - (x_3 - \hat{x}_3)] \right| \leq \frac{1}{r} (|x_2 - \hat{x}_2| + |x_3 - \hat{x}_3|) \leq \frac{2}{r} \bar{d}$$

Thus two fault detection rules can be formulated as:

$$1) \text{ trigger the fault alarm if } |y - \hat{y}| > \frac{2}{r} \bar{d}$$

$$2) \text{ trigger the fault alarm if } |\hat{\theta} - \bar{\theta}| > \Delta\theta_{\max}$$

Generally, the forms of tire faults can be divided into jump faults and shift faults, and these two fault situations can be judged by these two fault detection rules. When a jump tire fault occurs,  $|\theta_e| = |\hat{\theta} - \theta|$  will be abnormally larger than  $|\theta_e|_{\max}$  at the jump point for the outside disturbance is much larger than the limit of normal disturbance set before.

Thus, rule 1 is a sign of the jump faults. On the other hand, when a shift fault occurs,  $\hat{\theta}$  may track  $\theta$  very well but their values will be illogical, because  $\theta$  will exceed a logical limit  $(\bar{\theta} - \Delta\theta_{\max}, \bar{\theta} + \Delta\theta_{\max})$  for compensating for the continuous changes of parameters of the dynamic tire model. Thus, rules 2 will be triggered at this tire fault situation.

The following simulation results have proved the effectiveness of our tire fault observer.  $|\theta_e|_{\max}$ ,  $\bar{\theta}$ , and  $\Delta\theta_{\max}$  are determined by off-line experiments and a helpful Matlab toolbox that can be used to calculate matrixes  $L$ ,  $P$ , and  $Q$  is found in [10].

#### 4 Simulation Results

Using the data given in Table 1 and assuming  $r=0.2\text{m}$ ,  $m=5\text{Kg}$ ,  $J=0.25\text{Kgm}^2$ , and

$$F_n = 15\text{Kgm}^2/\text{s}^2, \text{ we can have } A = \begin{bmatrix} 0 & 0 & -20 \\ -9.8 & -4.9 & -50.96 \\ 12.86 & -4.9 & -66.88 \end{bmatrix}, B = \begin{bmatrix} -20 \\ -49 \\ -64.21 \end{bmatrix}, C =$$

$$\begin{bmatrix} 0 & 4 & -4 \end{bmatrix}. \text{ Choose } P = \begin{bmatrix} 1.0 & 0.1 & -0.3872 \\ 0.1 & 1.0 & -0.8552 \\ -0.3872 & -0.8552 & 0.8342 \end{bmatrix}, L = \begin{bmatrix} 5 \\ 0 \\ 5 \end{bmatrix}, Q =$$

$$\begin{bmatrix} -11.92 & -7.14 & 7.65 \\ -7.14 & -31.63 & 28.39 \\ 7.65 & 28.39 & -26.82 \end{bmatrix}. \text{ Then we can have } \lambda_{\max}(P) = 1.9, \lambda_{\min}(P) = 0.006, \lambda_{\min}(Q) =$$

0.67. Assuming  $|\theta_e|_{\max} = 0.2$ ,  $\bar{\theta} = 2.5$ ,  $\Delta\theta_{\max} = 2$ ,  $\tau = 0.1$ , and  $\gamma_1 = 20000$ ,  $\gamma_2 = 1$ , we have  $\bar{d} = 0.062$  and  $|y - \hat{y}| = 0.495$ .

Assume in the following simulation process that the value of  $\theta$  jumps from 1 to 3 at point  $t=5$ . Figures 2 and 3 show the values of  $y - \hat{y} = \omega - \hat{\omega}$ ,  $\theta$  and  $\hat{\theta}$ , respectively. From the Figure 2 we can find that  $y - \hat{y} = \omega - \hat{\omega}$  exceeds the threshold 0.495 immediately after  $t=5$ . It's obvious that the fault alarm 1 will be set in time.

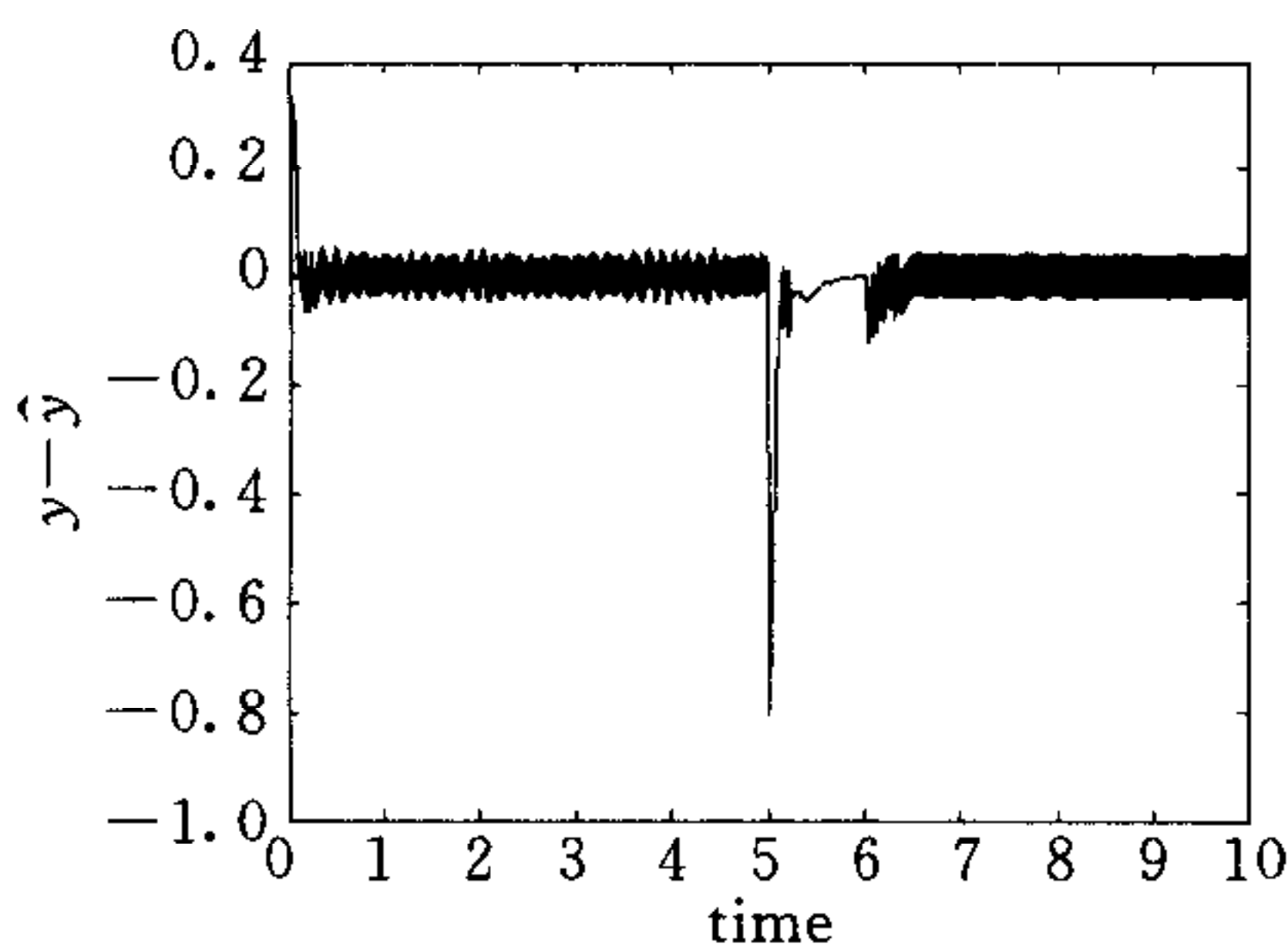


Fig. 2 Variation of  $y - \hat{y} = \omega - \hat{\omega}$  when the jump error occurs

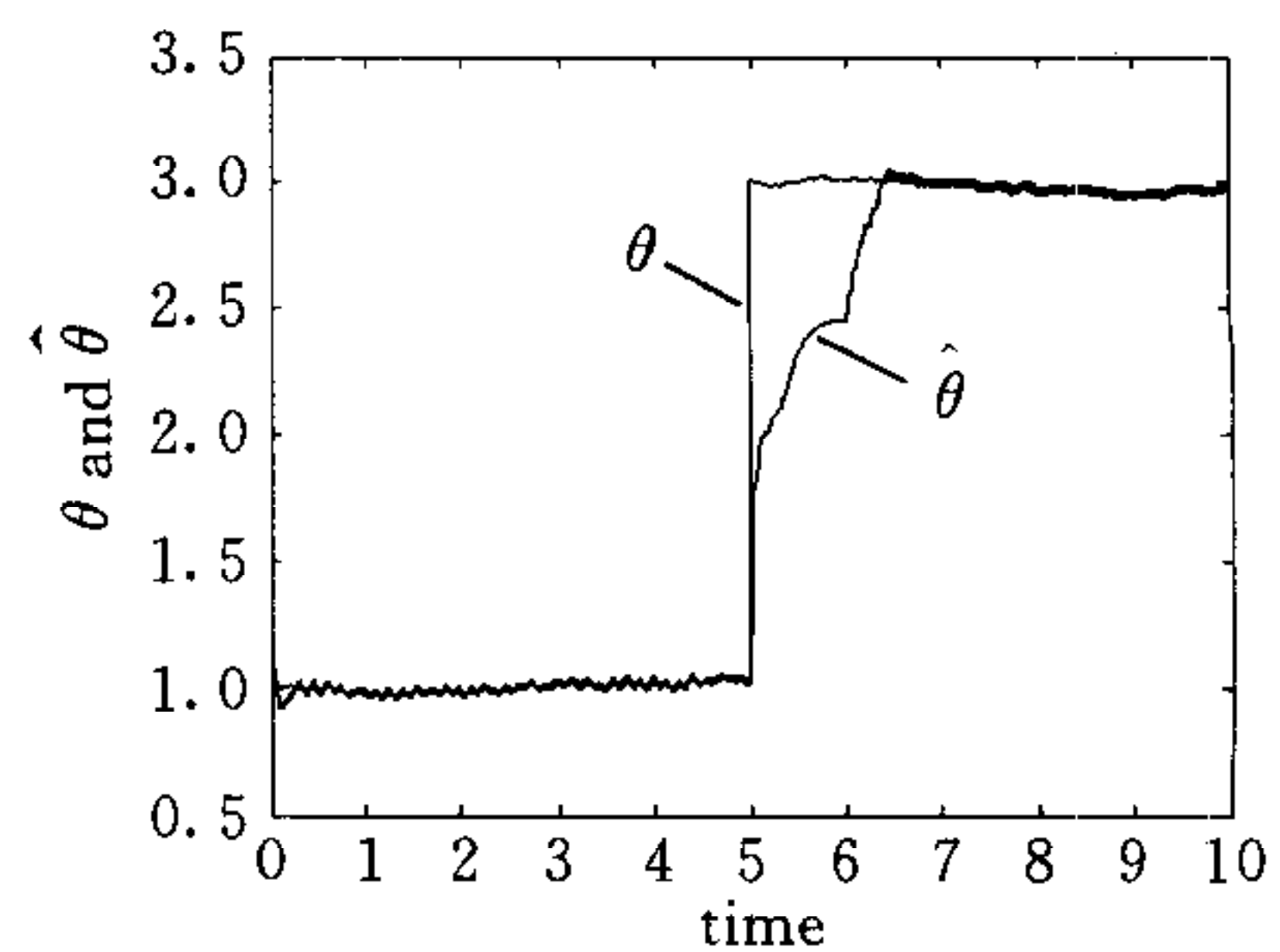


Fig. 3 Variation of  $\theta$  and  $\hat{\theta}$  when the jump error occurs

In the following simulation process, we assume that the value of  $\theta$  has an abnormal shift after  $t=5$ . Figures 4 and 5 show the values of  $y-\hat{y}=\omega-\hat{\omega}$ ,  $\theta$  and  $\hat{\theta}$ , respectively. From Figure 4 we can find that although  $y-\hat{y}=\omega-\hat{\omega}$  does not exceed the threshold 0.495 (only the statistic characteristics of the error output is changed), but  $\hat{\theta}$  keeps following  $\theta$  all the time as  $\theta$  increases continuously. It's obvious that the fault alarm 2 will act when  $\hat{\theta}$  become larger than  $\bar{\theta} + \Delta\theta_{\max}$ .

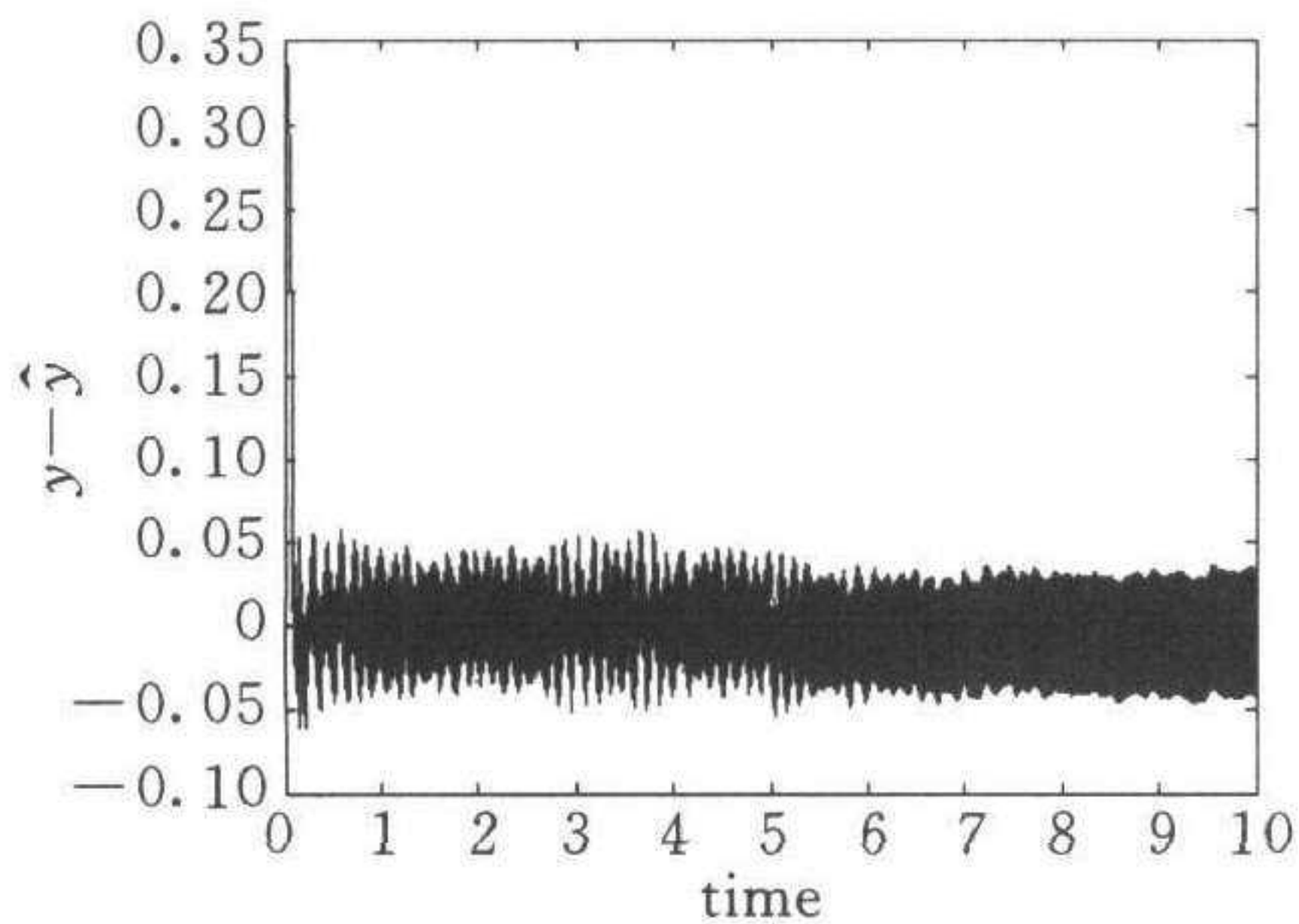


Fig. 4 Variation of  $y-\hat{y}=\omega-\hat{\omega}$  when the shift error occurs

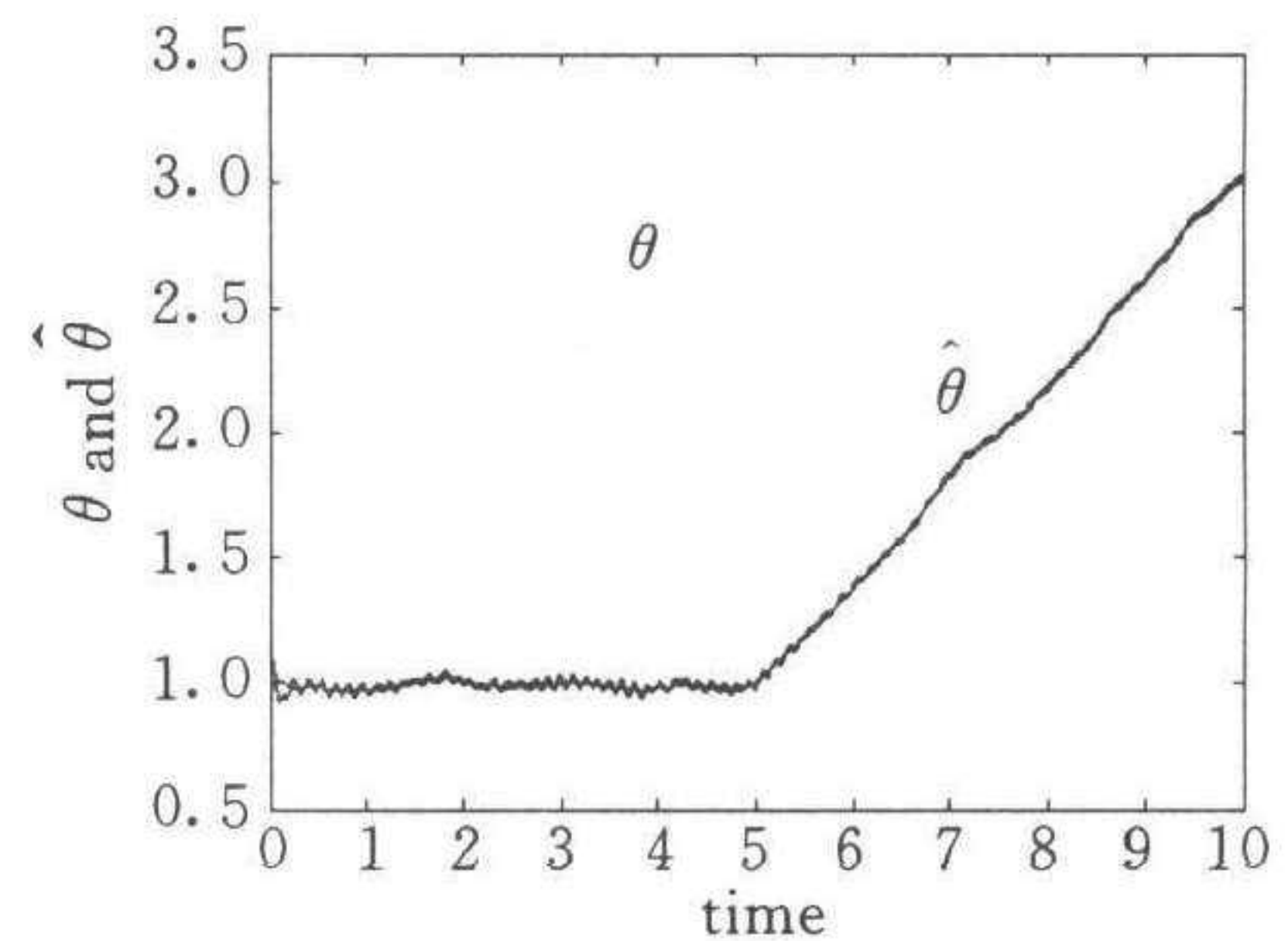


Fig. 5 Variation of  $\theta$  and  $\hat{\theta}$  when the shift error occurs

## 5 Conclusion

In this paper, we try to modify the LuGre model by introducing disturbance and discuss a fault observer for tire/road contact friction using only angular information on this modified model. The strong practically stable property of the estimated states and parameters has been proven. Based on this property, two fault detection rules are constructed and simulation results show the effectiveness of this method. We think that how to analyze the statistic characteristics of the error output so as to detect failure is a promising research direction and needs further discussion.

## References

- 1 Wang Fei-Yue, Shan Guo-Ling, Ding Yu-Hua, Li Li, Wang Zhi-Xue, Wang Chuan-Zhu, Feng Xi-Jin. Research in intelligent tire and its key technologies. *Rubber Industry Sinica*, 2002, **50**(12):713~719
- 2 Wang Fei-Yue, Wang Zhi-Xue, Li Li, Shan Guo-Ling, Wang Chuan-Zhu. The integrated triangle testbed system for intelligent tires and the corresponding research on its key technologies. *Tire Industry Sinica*, 2003, **23** (1): 10~15
- 3 Baker E, Nyborg L, Pacejka H. Tire modeling for use in vehicle dynamic studies. Society of Automotive Engineers Paper # 870421, 1987
- 4 Harned J, Johnston L, Scharpf G. Measurement of tire brake force characteristics as related to wheel slip (antiblock) control system design. *SAE Transactions*, 1969, **78**(690214):909~925
- 5 Canudas de Wit C, Olsson H, Astrom K J, Lischinsky P. A new model for control of systems with friction. *IEEE Transactions on Automatic Control*, 1995, **40**(3):419~425
- 6 Canudas de Wit C, Tsiotras P. Dynamic tire friction models for vehicle traction control. In: Proceedings of the 38th IEEE Conference on Decision and Control, 1999. 3746~3751
- 7 Canudas-de-Wit C, Horowitz R. Observers for tire/road contact friction using only wheel angular velocity information. In: Proceedings of the 38th IEEE Conference on Decision and Control, 1999. 3932~3937
- 8 Jingang Y, Alvarez L, Claeys X, Horowitz R, Canudas de Wit C. Emergency braking control with an observer-based dynamic tire/road friction model and wheel angular velocity information. In: Proceedings of the 2001 American Control Conference, 2001. 19~24
- 9 Young Man Cho, Rajamani R. A systematic approach to adaptive observer synthesis for nonlinear systems. *IEEE Transactions on Automatic Control*, 1997, **42**(4):534~537
- 10 El Ghaoui L, Nikoukhah R, Delebecque F. LMITOOL: A package for LMI optimization. In: Proceedings of the 34th IEEE Conference on Decision and Control, 1997. 3096~3101
- 11 Huang Lin. Stability Theory. Version 1. Beijing: Beijing University Press, 1992
- 12 Liao Xiao-Xin. Stability's Theory, Method and Applications. Version 1. Wuhan: Huazhong University of Science and Technology Press, 1999

**LI Li** Received his master degree from the Huazhong University of Science and Technology, P. R. China, in 2001. Now he is studying at Systems and Industrial Engineering Department of University of Arizona. His research interests include artificial intelligence, intelligent controls and nonlinear complex systems.

**WANG Fei-Yue** Received his master degree from Zhejiang University, Hangzhou, P. R. China, and the Ph. D. degree in Computer and Systems Engineering from Rensselaer Polytechnic Institute, Troy, NY, in 1984 and 1990, respectively. Now He is a professor of Systems and Industrial Engineering at University of Arizona, USA and also the director of Complex Systems and Intelligent Science Laboratory, Institute of Automation, Chinese Academy of Sciences. His research interests include modeling, analysis and control of complex systems. Currently, Dr. Wang is the secretary-Elect of the IEEE ITS Council, associate editor of the IEEE Transactions on Robotics and Automation, SMC, ITS and editor in charge of the World Scientific Series on Intelligent Control and Intelligent Automation.

**SHAN Guo-Ling** The vice-president and chief engineer of Triangle Tire Corporation, Ltd, WeiHai, Shandong, P. R. China.

**ZHOU Qun-Zhi** Received his bachelor degree from Tsinghua University, P. R. China. He is currently studying at Complex Systems and Intelligent Science Laboratory, Institute of Automation, Chinese Academy of Sciences. His research interests include intelligent controls, nonlinear systems, and data fusion.

## 基于轮胎/路面磨擦状况估计的轮胎故障观测器设计

李力<sup>1,3</sup> 王飞跃<sup>1,3</sup> 单国玲<sup>2</sup> 周群植<sup>1</sup>

<sup>1</sup>(中国科学院自动化研究所复杂系统和智能科学实验室 北京 100080)

<sup>2</sup>(中国山东威海三角轮胎股份有限公司 威海 210016)

<sup>3</sup>(美国亚利桑那大学 PARCS 研究中心 图森 亚利桑那州)

(E-mail: lil@email.arizona.edu)

**摘要** 轮胎故障是造成交通事故的主要原因之一. 但是目前大多数轮胎故障监测方法由于需要使用各种复杂的传感器因此制造代价高昂且不可靠. 为此, 提出了一种新型实用的轮胎故障观测器. 基于考虑外界不确定干扰的新型动态轮胎/路面磨擦模型, 该观测器仅仅使用汽车驱动力及轮胎转速数据, 跟踪估计轮胎/路面磨擦系数的变化, 并通过对磨擦状况的分析对轮胎状态做出合理的判断. 由于转速传感器是汽车防滑刹车控制系统 (ABS) 的基本组成部分, 因此该观测器可与 ABS 结合工作, 低成本的实现轮胎故障监测.

**关键词** 轮胎/路面磨擦估计, 非线性观测器, 强实用稳定性, 故障观测器

**中图分类号** TP206.3